

## **Quantitative ultrasonic tissue characterization with real-time integrated backscatter imaging in normal human subjects and in patients with dilated cardiomyopathy\***

ZVI VERED, M.D., BENICO BARZILAI, M.D., G. A. MOHR, PH.D., LEWIS J. THOMAS III, PH.D., RANDALL GENTON, M.D., BURTON E. SOBEL, M.D., THOMAS A. SHOUP, PH.D., H. E. MELTON, PH.D., JAMES G. MILLER, PH.D., AND JULIO E. PÉREZ, M.D.

**ABSTRACT** We have shown previously that the physical properties of myocardium in dogs can be characterized with quantitative ultrasonic integrated backscatter and that interrogation of the tissue with ultrasound can delineate cardiac cycle-dependent changes in ultrasonic backscatter in normal tissue that disappear with ischemia and reappear with reperfusion if functional integrity is restorable. To determine whether this approach can be applied to man, we implemented an automatic gain compensation and continuous data acquisition system to characterize myocardium with quantitative ultrasonic backscatter and to detect cardiac cycle-dependent changes in real time. We developed a two-dimensional echocardiographic system with quantitative integrated backscatter imaging capabilities for use in human subjects that can automatically differentiate ultrasonic signals from blood as opposed to those obtained from tissue and adjust the slope of the gain compensation appropriately. Real-time images were formed from a continuous signal proportional to the logarithm of the integrated backscatter along each A-line. In our initial investigation, 15 normal volunteers (ages 17 to 40 years, heart rates 44 to 88 beats/min) and five patients with dilated cardiomyopathy (ages 22 to 52, heart rates 82 to 120 beats/min) were studied with conventional parasternal long-axis echocardiographic views. Diastolic-to-systolic variation of integrated backscatter in the interventricular septum and left ventricular posterior wall was seen in each of the normal subjects averaging  $4.6 \pm 1.4$  dB (SD) and  $5.3 \pm 1.5$  dB ( $n = 127$  sites), respectively. In patients with dilated cardiomyopathy, the magnitude of this variation was either reduced or absent, averaging  $0.9 \pm 0.8$  dB in the interventricular septum and  $1.8 \pm 1.2$  dB in the left ventricular posterior wall ( $n = 31$  sites;  $p < .01$  for both). In eight of the 31 sites in myopathic hearts, no variation was detectable. The results obtained demonstrate that quantitative ultrasonic tissue characterization is feasible in man. Real-time integrated backscatter imaging delineates cardiac cycle-dependent changes in normal human myocardium and quantitatively differentiates between normal and myopathic myocardium. This system offers promise for the quantitative, diagnostic detection of diverse disease processes, including myocardial ischemia and responses of the tissue to reperfusion.

*Circulation* 76, No. 5, 1067-1073, 1987.

From the Departments of Medicine and Physics, Washington University School of Medicine, St. Louis, and Hewlett-Packard, Andover, MA.

Supported in part by NIH grants HL-17646 (SCOR in Ischemic Heart Disease), R236733, and RR01362.

Address for correspondence: Julio E. Pérez, M.D., Cardiovascular Division, Washington University School of Medicine, 660 S. Euclid Ave., Box 8086, St. Louis, MO 63110.

Received Jan. 14, 1987; revision accepted Aug. 6, 1987.

\*All editorial decisions for this article, including selection of reviewers and the final disposition, were made by a guest editor. This procedure applies to all manuscripts with authors from the Washington University School of Medicine.

WE HAVE SHOWN previously that myocardial tissue characterization with ultrasonic integrated backscatter permits delineation of physiologic and pathologic changes in heart muscle in vitro and in vivo.<sup>1, 2</sup> In addition, we have found that normal canine myocardium exhibits cardiac cycle-dependent variation of integrated backscatter indicative of sequential and systematic changes in physical properties of the tissue. The cyclic variation of integrated backscatter has been shown to be a sensitive measure of intrinsic acoustic

properties of the tissue rather than its dimensions<sup>3-5</sup> and delineates quantitative differences between acoustic properties of irreversibly injured and normal myocardium and changes in reversibly injured tissue that regress with reperfusion.<sup>6, 7</sup> The overall objective of our studies in experimental animals has been the development and validation of an approach to tissue characterization that would ultimately permit noninvasive diagnostic delineation of specific cardiomyopathic states of diverse etiologies and the differentiation of reversible from irreversible myocardial ischemic injury. A real-time integrated backscatter imaging system was developed and used in the present study to determine whether it could delineate cardiac cycle-dependent changes in integrated backscatter in hearts of normal human subjects and quantitatively differentiate acoustic properties of normal myocardium from those in patients with dilated cardiomyopathy. The specific objectives were: (1) demonstration of the feasibility of the approach with radiofrequency-derived integrated backscatter in human subjects; (2) acquisition of data typical of normal myocardium that could serve as baseline information needed for interpretation of results of future studies, and (3) characterization of diffuse cardiomyopathic changes and comparison with data obtained from normal subjects.

## Methods

**Ultrasonic system.** The real-time, two-dimensional imaging system developed uses a modified commercially available imager with a 64-channel phased-array transducer operating at 3.5 MHz. A block diagram of the conventional imaging system is shown in figure 1. A conventional 90 degree sector image is formed at a rate of 30 Hz. On reception, the signal from each

element of the array is amplified, mixed to an appropriate intermediate frequency (IF), phased, delayed, and summed with the signals from all other elements. Summed IF signals are used to produce a video signal that is filtered to enhance the image, digitized, and passed to the scan converter. The scan converter transforms the data from their original polar coordinates to a TV raster format and overlays the various graphics in the final display.

The modifications introduced in the processing path used for integrated backscatter imaging are depicted in figure 2. The initial process of mixing, delaying, and summing is the same as for the case of conventional two-dimensional imaging except for inclusion of rational gain compensation (RGC). In conventional time-gain compensation, values for the compensation factor are determined only by the depth into the tissue without respect to the structures encountered along individual lines. In contrast, RGC is a form of automatic gain compensation that uses the magnitude of the returned echo to identify the source of the echo as either in tissue or in blood and adjusts the slope of the gain compensation accordingly on a line-by-line basis.<sup>8</sup> This gain compensation scheme, as opposed to conventional time-gain compensation, minimizes differences in absolute signal levels in comparisons of echoes from one region of the heart with those from adjacent regions.

Once the summed IF signal has been formed, it can be sent to either the video processing path or the integrated backscatter processor. This processor incorporates digital hardware clocked at a rate of 10 MHz that implements our previously described approach<sup>9, 10</sup> to produce a continuous signal that is proportional to the logarithm of integrated backscatter along each acoustic line in the image. The integration time is 3.2  $\mu$ sec, and the dynamic range of the integrated backscatter processor is greater than 40 dB. The full dynamic range of the integrated backscatter data is linearly mapped in 0.5 dB increments into the approximately 30 dB dynamic range available in the displayed video images. The output of the processor then follows the remaining signal path through the scan converter as in conventional imaging.

The present investigation focuses on the magnitude of the cyclic variation as opposed to the time-averaged value of integrated backscatter. The magnitude of cyclic variation in a specific site of analysis is defined quantitatively (in dB) as the logarithm of the ratio of the backscattered energies at diastole

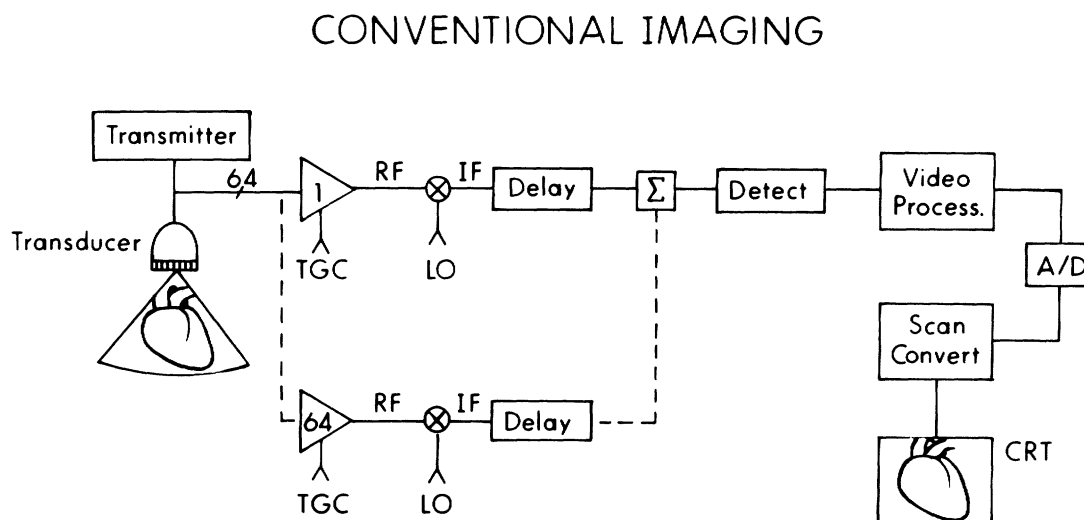


**FIGURE 1.** Diagram showing the processing sequence with the two-dimensional phased-array imaging system. The signal from each element is amplified, mixed to an intermediate frequency (IF), phased, delayed, and summed with other elements. IF signals are then detected to yield a video signal, which is then filtered, digitized, and transmitted to the scan converter.

## INTEGRATED BACKSCATTER IMAGING

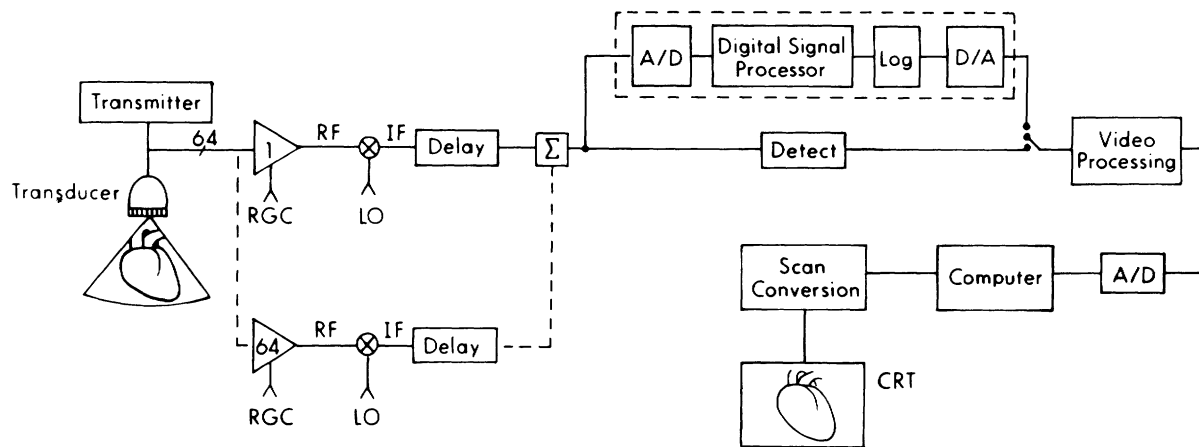


**FIGURE 2.** Diagram showing the processing path for integrated backscatter imaging. The only modification compared with conventional imaging before summation is the use of rational gain compensation (RGC). Once the summed IF signal has been formed, it can be steered to the conventional imaging path or to the integrated backscatter processor.

and systole. Over the range of transmit power employed (settings between 30 and 40 dB), adjusted individually for each subject and patient, the magnitude of cyclic variation (in dB) is essentially independent of transmit power. Absolute calibration of the time-averaged integrated backscatter expressed relative to the reflection from a steel plate is not available in the present implementation. However, ratios of time-averaged integrated backscatter (such as increased backscatter in zones of scar) are available quantitatively (in dB) as the logarithm of the ratio of the backscattered energies in the zones being compared.

The digitized image data (which represent integrated backscatter) are transmitted to a computer that can record up to 4 megabytes of data in real time, yielding storage of 88 frames of data corresponding to approximately 3 sec. In some applications, the area of the frame stored in the computer is limited to a particular region of interest, so that the total number of frames recorded can be increased.

As many as three channels of physiologic signals such as pressure and electrocardiogram (ECG) are multiplexed into the computer at the start of each line in the image. This yields an approximately 3.5 kHz sampling rate for the physiologic signals. Thus physiologic data are also collected in real time. After the computer has received the backscatter image, it is passed to the scan converter for processing and display as in conventional systems. Because all the modifications required for integrated backscatter processing fit into the processing pipeline used for conventional imaging, the system runs in real time for conventional imaging, integrated backscatter imaging and data collection.

**Subjects.** Fifteen healthy male volunteers ages 17 to 40 years ( $32 \pm 5$  [SD]) and five patients with dilated cardiomyopathy, three men and two women ages 22 to 52 ( $37 \pm 13$ ) were studied. Each subject underwent ultrasonic imaging with a 3.5 MHz transducer on a 30 to 45 degree left lateral position with the ECG recorded simultaneously. First, conventional two-dimensional echocardiographic images were obtained from the parasternal and apical views. Gross cardiac abnormalities were excluded in the normal subjects and the diagnosis of dilated cardiomyopathy was confirmed in the patients. Each patient had evidence of significant chamber enlargement with diffuse hypocontractility

of the ventricles. The etiology of the cardiomyopathy was idiopathic in four and ischemic in one of the patients. They were all symptomatic, and four of them were awaiting cardiac transplantation. The system was then switched to integrated backscatter imaging. In each subject, three to four images in the parasternal long-axis view were obtained in a single step by placing a computer-generated region of interest over the interventricular septum. This procedure was repeated for the left ventricular posterior wall. Each series of images (30 frames/sec) contained two to six cardiac cycles depending on the subject's heart rate. Digitized data from regions of interest were stored for subsequent analysis.

**Analysis of ultrasonic data.** Data analysis of the computer-stored regions of interest was performed by selecting a site of analysis approximately  $20 \times 8$  mm, which excluded both endocardial and epicardial specular reflections in an end-diastolic frame. One to three intramyocardial sites were selected in each image. Sites of analysis were selected based on adequate visualization of both endocardium and epicardium. Data analysis throughout the cardiac cycle was achieved by frame-by-frame tracking of the desired site of myocardium and adjusting the location of the site of analysis accordingly, keeping it well within the myocardium with its dimensions constant (figure 3). The spatially averaged integrated backscatter from each site (in dB) was generated and displayed by the computer along with the ECG as a function of time in graphic form (figure 4). The average cardiac cycle-dependent change in integrated backscatter, defined as the average difference between late diastolic and late systolic values (in dB) was calculated for all sites for each subject. In addition, cyclic variation in the septum and in the posterior wall was compared between normals and patients with cardiomyopathy. A limited evaluation of intraobserver and interobserver variability was performed by repeated analysis of randomly selected sites. All images were obtained by one of the authors, whereas all other steps of analysis were carried out independently by four investigators. Interobserver variation was evaluated by comparing the results of analysis obtained by three independent observers.

**Statistics.** Values are expressed as mean  $\pm$  SD. Statistical analysis was carried out based on the unpaired t test.

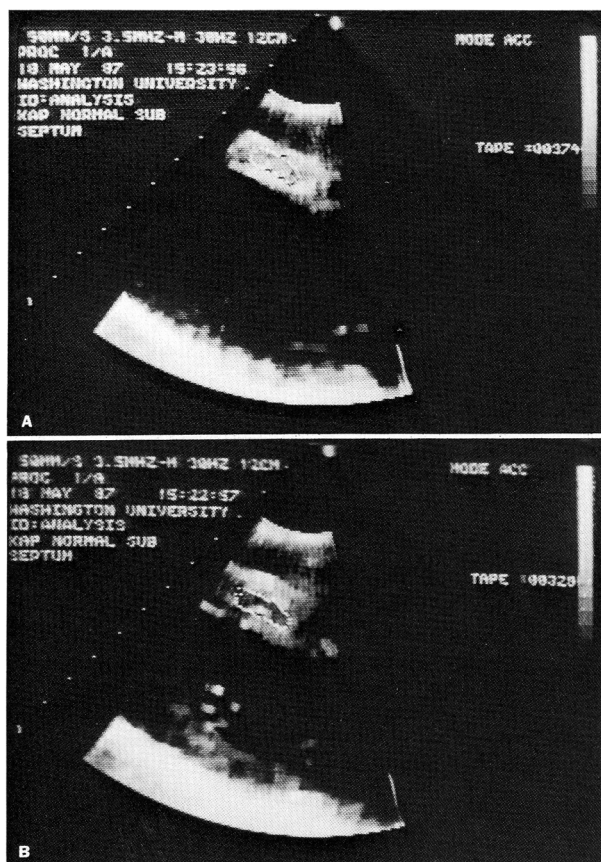


**FIGURE 3.** A, End-diastolic frame from a normal subject. The site of analysis is in the interventricular septum. Note the relatively bright myocardial echoes characteristic of this portion of the cardiac cycle. B, End-systolic frame. Note the relative decrease of integrated backscatter in systole (cardiac cycle-dependent variation of integrated backscatter).

## Results

Clinical information and mean values of integrated backscatter measured in the 15 normal subjects and in the five patients with dilated cardiomyopathy are shown in table 1. Conventional echocardiographic images were considered to be of good quality in eight normal volunteers, of average quality in five, and of below-average quality in two. Images were judged good in two patients with dilated cardiomyopathy and average in three. Diastolic-to-systolic cyclic variation of backscatter was present in each of the normal subjects (table 1, figure 3). It was detected readily in the posterior wall of 13 and in the septum of 10 of the 15 normal subjects. It was detected to a lesser extent in the posterior wall of two and in the septum of five subjects. It was detectable in all 127 sites. The mean of the cardiac cycle-dependent variation of integrated backscatter from all sites was  $5.3 \pm 1.5$  dB (SD) in the posterior wall and  $4.6 \pm 1.4$  dB in the septum.

Cyclic variation of backscatter was significantly

reduced in all patients with dilated cardiomyopathy, averaging  $1.8 \pm 1.2$  dB in the left ventricular posterior wall and  $0.9 \pm 0.8$  dB in the septum ( $n = 31$  sites;  $p < .01$  for both) (figures 4 and 5). In eight of the 31 sites in myopathic hearts no variation was detectable.

The limited evaluation of intraobserver variability yielded differences of less than 1 dB; interobserver variation was less than 1.4 dB (figure 6).

## Discussion

Cardiac cycle-dependent variation of integrated backscatter reflects physiologic changes in acoustic properties of specific regions of normal canine myocardium. Thus quantitative differences in the amplitude of cycle-dependent variation of integrated backscatter have been found among the base, midwall, and apex of normal canine myocardium.<sup>5</sup> These differences may be associated with corresponding regional differences in contractile performance described by others.<sup>11</sup> We have shown previously that cardiac cycle-dependent variation of integrated backscatter is blunted within 5 min after the onset of ischemia and is restored after reperfusion.<sup>7, 12</sup> The changes in cyclic variation occur

**TABLE 1**

**Integrated backscatter in normal subjects vs patients with dilated cardiomyopathy**

| No. | Subject | Age (yr) | Heart rate (beats/min) | Mean integrated backscatter (dB $\pm$ SD) |                  |
|-----|---------|----------|------------------------|---|------------------|
|     |         |          |                        | IVS                                       | PW               |
| 1   | N       | 34       | 51                     | $5.0 \pm 1.4$                             | $6.0 \pm 1.1$    |
| 2   | N       | 33       | 68                     | $4.7 \pm 0.7$                             | $4.0 \pm 0.5$    |
| 3   | N       | 34       | 64                     | $6.4 \pm 0.7$                             | $6.4 \pm 0.4$    |
| 4   | N       | 17       | 68                     | $4.0 \pm 0.8$                             | $4.7 \pm 0.7$    |
| 5   | N       | 32       | 67                     | $5.8 \pm 0.7$                             | $7.0 \pm 0.8$    |
| 6   | N       | 36       | 57                     | 2.9 <sup>A</sup>                          | $7.5 \pm 0.9$    |
| 7   | N       | 31       | 53                     | $5.6 \pm 0.5$                             | $6.3 \pm 0.4$    |
| 8   | N       | 32       | 44                     | $3.5 \pm 0.5$                             | $4.7 \pm 0.5$    |
| 9   | N       | 34       | 63                     | $6.1 \pm 0.6$                             | $6.5 \pm 0.6$    |
| 10  | N       | 40       | 88                     | $3.5 \pm 0.1$                             | $4.1 \pm 0.6$    |
| 11  | N       | 32       | 72                     | $3.0 \pm 0.7$                             | $2.3 \pm 0.4$    |
| 12  | N       | 29       | 76                     | $2.7 \pm 0.2$                             | 6.5 <sup>A</sup> |
| 13  | N       | 30       | 72                     | $3.3 \pm 1.1$                             | $4.6 \pm 0.4$    |
| 14  | N       | 31       | 82                     | $3.9 \pm 0.9$                             | $3.4 \pm 0.4$    |
| 15  | N       | 33       | 76                     | $2.7 \pm 0.4$                             | $3.6 \pm 1.3$    |
| 1   | DC      | 50       | 112                    | $1.6 \pm 0.4$                             | 0                |
| 2   | DC      | 52       | 92                     | $0.6 \pm 0.8$                             | 1.2 <sup>A</sup> |
| 3   | DC      | 23       | 120                    | $0.7 \pm 0.2$                             | $2.1 \pm 0.4$    |
| 4   | DC      | 34       | 88                     | $1.6 \pm 0.4$                             | $1.8 \pm 0.5$    |
| 5   | DC      | 28       | 82                     | 0   | $3.1 \pm 0.8$    |

Intraobserver variability estimated less than 1 dB; interobserver variability estimated less than 1.4 dB.

N = normal; DC = dilated cardiomyopathy; IVS = interventricular septum; PW = posterior wall.

<sup>A</sup>One measurement only.

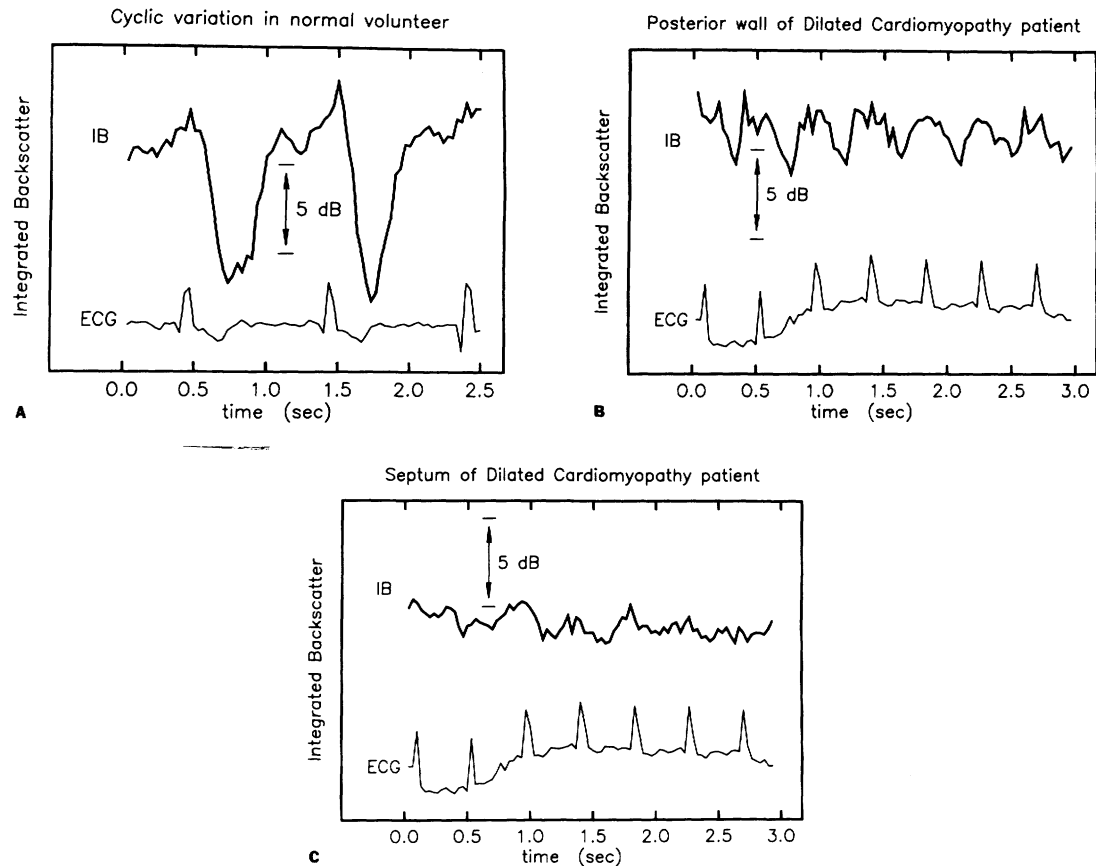


**FIGURE 4.** A, Hard copy recording from a posterior wall site in a normal volunteer, demonstrating the diastolic-to-systolic variation of integrated backscatter. Note the marked decrease occurring during cardiac systole. B, Hard copy recording from a posterior wall site in a patient with dilated cardiomyopathy, demonstrating reduced cyclic variation of integrated backscatter. C, Hard copy recording from the interventricular septum of the same patient as in B, demonstrating markedly reduced cyclic variation of integrated backscatter. The value of cyclic variation measured in this site was 0.7 dB.

promptly after ischemia and appear to be a particularly sensitive acoustic property associated with the contractile performance of tissue and its impairment by ischemia.<sup>12</sup> Zones of remote myocardial infarction of canine myocardium lose cyclic variation of integrated backscatter permanently.<sup>6, 13</sup>

Several other investigators, using alternative methods, have confirmed the presence of cardiac cycle-dependent variation of backscatter in normal myocardium. To determine whether qualitatively similar phenomena could be recognized in man, Olshansky et al.<sup>14</sup> have used regional average gray-level detection by digitizing two-dimensional images obtained with a commercial phased-array scanner on 16 normal human individuals. In six, images were digitized from stop-frame photographs. Ten images were acquired in digital format from the scanner. Average gray level was measured in portions of left ventricular posterior wall in the parasternal long-axis view. Both methods revealed significant higher average gray levels at end-

diastole than at end-systole. More recently, others<sup>15-17</sup> obtained analogous results with different methods.

In the present study, cardiac cycle-dependent variation of the actual radiofrequency-derived backscatter was delineated in human subjects quantitatively in real-time, two-dimensional imaging for the first time. Because our technique is based on the unprocessed radiofrequency ultrasonic signals, allowing quantification based on the energy returned from a local volume of tissue, we believe that integrated backscatter measurements may provide a more robust diagnostic tool than gray-level analysis of processed video images. The results obtained demonstrate that cardiac cycle-dependent variation of integrated backscatter in man can be quantified *in vivo*. Furthermore, normal myocardium can be quantitatively differentiated from myopathic hearts, and hence real-time quantitative delineation of backscatter for diagnostic purposes is feasible.

Cardiac cycle-dependent variation of integrated

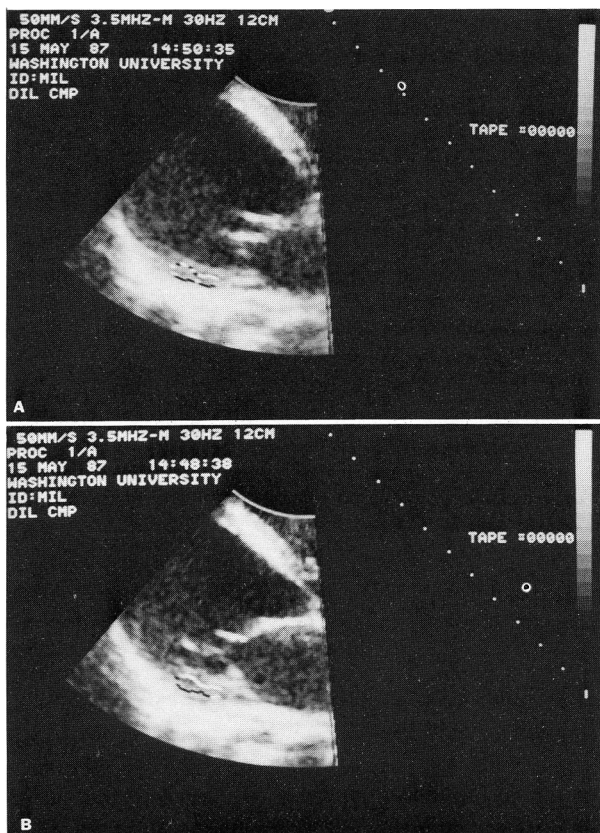


**FIGURE 5.** A, End-diastolic frame from a patient with dilated cardiomyopathy. The site of analysis is in the left ventricular posterior wall. B, End-systolic frame. Note the modest degree of cyclic variation as compared with the normal subject in figure 3.

backscatter was observed on the real-time images and was quantitatively detectable in each of the 15 subjects. It was significantly reduced in patients with dilated cardiomyopathy. Although many of the subjects included in this study were relatively young, the distribution of quality of conventional echocardiographic images obtained was typical of that in most populations evaluated in clinical adult echocardiography laboratories. Quantitative integrated backscatter imaging at the present time requires adequate conventional ultrasonic images.

The mechanism for the reduction in cyclic variation of integrated backscatter in myopathic hearts is not yet clear. We have shown previously that subepicardial regions in myocardium from open-chest dogs exhibit reduced cyclic variation that parallels their contractile performance.<sup>18</sup> Thus it is possible that reduced mechanical function in patients with dilated cardiomyopathy is in part responsible for the observed reduced cyclic variation. However, the role of myocardial fibrosis in this patient population cannot be excluded as an additional determinant. The availability of absolute calibration in future systems to allow mea-

surements of time-averaged integrated backscatter may permit the elucidation of these differences. We have demonstrated previously that time-averaged integrated backscatter sensitively detects myocardial ischemia and infarction in open- and closed-chest dogs.<sup>6, 12, 19</sup> Evaluation of this variable is likely to be useful for detection of diffuse changes<sup>20, 21</sup> such as those associated with rejection of cardiac allografts. The present system requires adjustment of rational gain compensation for each subject at the time of each examination. Standardization for time-average integrated backscatter from patient to patient has not yet been achieved, primarily because an appropriate reflector for reference in vivo has not yet been identified. The approach suggested by Tanaka, Gibson, and their collaborators<sup>22-24</sup> employing the bright echos from the pericardium, or the use of echoes from the lung,<sup>25</sup> may be useful for standardizing signals.

The basis for the difference between cardiac cycle-dependent variation of integrated backscatter in the interventricular septum and posterior wall of both normal and myopathic hearts is not clear. It may reflect only technical features of ultrasonic imaging. Integrated backscatter imaging of the septum in some subjects magnifies the presence of a longitudinal band of echoes, "brighter" than the surrounding myocardium, often noticed during conventional imaging in both

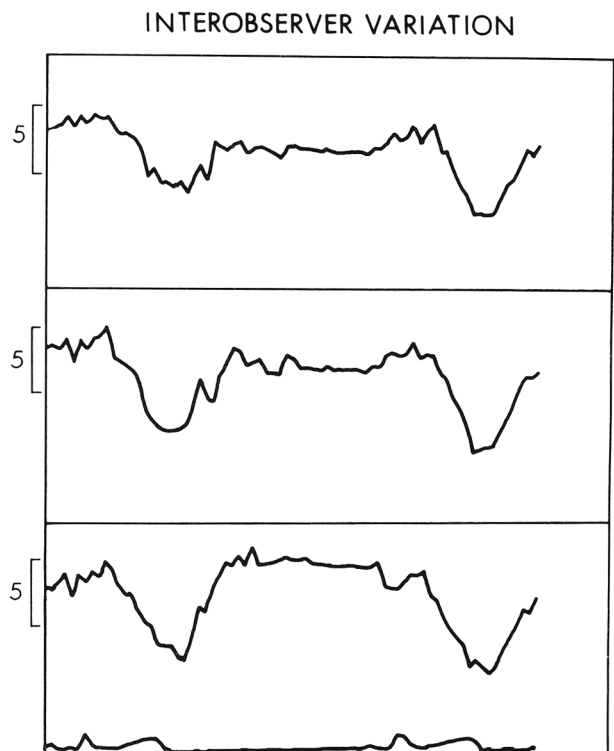


**FIGURE 6.** Analysis of results from one site in a normal subject by three independent observers.

long-axis and apical four-chamber views. Such echos may become more pronounced during cardiac systole. When this is the case (as occurred in five of our 15 subjects), the spatially averaged integrated backscatter in systole is increased, minimizing the cardiac cycle-dependent variation. Such echoes may represent changes in fiber orientation within the cardiac muscle. Results of previous studies from our laboratory have indicated<sup>26, 27</sup> that fiber orientation is an important determinant of both ultrasonic backscatter and attenuation in myocardium. In the present study, data were obtained from parasternal long-axis views only. Judging from preliminary observations in a limited number of patients, we believe that the longitudinal band of echoes is particularly pronounced in the apical four-chamber view, especially in patients with myocardial hypertrophy.

Results of this study indicate that quantitative integrated backscatter imaging is feasible in man. It offers quantitative noninvasive differentiation between acoustic properties of normal and cardiomyopathic heart muscle. The system should allow quantitative differentiation between various disease states and normal myocardium in patients.

We are grateful for the excellent secretarial assistance and patience of Mrs. Barbara Donnelly and Mrs. Kelly Hall.

## References

1. Miller JG, Perez JE, Sobel BE: Ultrasonic characterization of myocardium. *Prog Cardiovasc Dis* **28**: 85, 1985
2. Miller JG, Perez JE, Madaras EI, Mottley JG, Johnston PH, Blodgett ED, Thomas LJ, Sobel BE: Myocardial tissue characterization: an approach based on quantitative backscatter and attenuation. *Proc 1983 IEEE Ultrasonics Symp* **83CH1947-1**: 782, 1983
3. Madaras EI, Barzilai B, Pérez JE, Sobel BE, Miller JG: Changes in myocardial backscatter throughout the cardiac cycle. *Ultrason Imaging* **5**: 229, 1983
4. Barzilai B, Madaras EI, Sobel BE, Miller JG, Pérez JE: Effects of myocardial contraction on ultrasonic backscatter before and after ischemia. *Am J Physiol* **247**: H478, 1984
5. Mottley JG, Glueck RM, Pérez JE, Sobel BE, Miller JG: Regional differences in the cyclic variation of myocardial backscatter that parallel regional differences in contractile performance. *J Acoust Soc Am* **76**: 1617, 1984
6. Thomas LJ III, Barzilai B, Wickline SA, Gessler CG, Sobel BE, Pérez JE, Miller JG: Real-time, two-dimensional imaging based on quantitative integrated backscatter. *Ultrason Imaging* **8**: 36, 1986 (abst)
7. Glueck RM, Mottley JG, Miller JG, Sobel BE, Pérez JE: Effect of coronary artery occlusion and reperfusion on cardiac cycle-dependent variation of myocardial ultrasonic backscatter. *Circ Res* **56**: 683, 1985
8. Melton HE, Skorton DJ: Rational gain compensation for attenuation in cardiac ultrasonography. *Ultrason Imaging* **5**: 214, 1983
9. O'Donnell M, Bauwens D, Mimbs JW, Miller JG: Broadband integrated backscatter: an approach to spatially localized tissue characterization in vivo. *Proc IEEE symp* **79CH1482-9**: 175, 1979
10. Pérez JE, Madaras EI, Sobel BE, Miller JG: Quantitative myocardial characterization with ultrasound. *Automedica* **5**: 209, 1984
11. Haendchen RV, Wyatt HL, Maurer G, Zwehl W, Baer M, Meerbaum S, Corday E: Quantitation of regional function by two-dimensional echocardiography. I. Patterns of contraction in the normal left ventricle. *Circulation* **67**: 1234, 1983
12. Wickline SA, Thomas LJ III, Miller JG, Sobel BE, Pérez JE: Sensitive detection of the effects of reperfusion on myocardium by ultrasonic tissue characterization with integrated backscatter. *Circulation* **74**: 389, 1986
13. Thomas LJ III, Barzilai B, Sobel BE, Pérez JE, Miller JG: Quantitative real-time ultrasonic backscatter imaging of normal myocardium and infarct in closed-chest dogs. *Circulation* **74**(suppl II): II-270, 1986 (abst)
14. Olshansky B, Collins SM, Skorton DJ, Prasad NV: Variation of left ventricular myocardial gray level on two-dimensional echocardiograms as a result of cardiac contraction. *Circulation* **70**: 972, 1984
15. Angerman CE, Hart RJ, Stemfle U, Zwehl W, Theisen K: Frame by frame quantitation of myocardial backscatter: analysis of standard 2D echo images and radio frequency signals. *Circulation* **74**(suppl II): II-270, 1986 (abst)
16. Chandrasekaran K, Chu A, Greenleaf JF, Bahn RC, Edwards WD, Seward JB, Tajik AJ: 2D echo quantitative texture analysis of acutely ischemic myocardium. *Circulation* **74**(suppl II): II-271, 1986 (abst)
17. Sagar KB, Rhyne TL, Warltier DC, Pelc L, Wann LS: Intramyocardial variability in integrated backscatter: effects of coronary artery occlusion and reperfusion. *Circulation* **75**: 436, 1987
18. Wickline SA, Thomas LJ III, Miller JG, Sobel BE, Pérez JE: The dependence of myocardial ultrasonic integrated backscatter on contractile performance. *Circulation* **72**: 189, 1985
19. Mimbs JW, Bauwens D, Cohen RD, O'Donnell M, Miller JG, Sobel BE: Effects of myocardial ischemia on quantitative ultrasonic backscatter and identification of responsible determinants. *Circ Res* **49**: 89, 1981
20. Pérez JE, Barzilai B, Madaras EI, Glueck RM, Saffitz JE, Johnston P, Miller JG, Sobel BE: Applicability of ultrasonic tissue characterization for longitudinal assessment and differentiation of calcification and fibrosis in cardiomyopathy. *J Am Coll Cardiol* **4**: 88, 1984
21. Mimbs JW, O'Donnell M, Miller JB, Sobel BE: Detection of cardiomyopathic changes induced by doxorubicin based on quantitative analysis of ultrasonic backscatter. *Am J Cardiol* **47**: 1056, 1981
22. Tanaka M, Terasawa Y, Hikichi H: Qualitative evaluation of the heart tissue by ultrasound. *J Cardiogr* **7**: 515, 1977
23. Hikichi H, Tanaka M: Ultrasono-cardiotomographic evaluation of histologic changes in myocardial infarction. *Jpn Heart J* **22**: 287, 1981
24. Logan-Sinclair RB, Wong CM, Gibson DG: Clinical applications of amplitude processing of echocardiographic images. *Br Heart J* **45**: 621, 1981
25. Rhyne TL, Sagar KB, Wann SL, Haasler G: The myocardial signature: absolute backscatter, cyclical variation frequency variation and statistics. *Ultrason Imaging* **8**: 107, 1986
26. Mottley JG, Miller JG: Anisotropy of ultrasonic backscatter in canine myocardium: theory and results in vitro. *Ultrason Imaging* **8**: 34, 1986 (abst)
27. Madaras EI, Pérez JE, Sobel BE, Miller JG: Anisotropy of ultrasonic backscatter in canine myocardium: results in vivo. *Ultrason Imaging* **8**: 35, 1986 (abst)